Journal of Applied Physics

Shear response of magnetorheological fluid with $Zn_{0.2}Fe_{2.8}O_4$ sub-micron hollow spheres

Cite as: J. Appl. Phys. **129**, 033901 (2021); https://doi.org/10.1063/5.0031536
Submitted: 01 October 2020 . Accepted: 20 December 2020 . Published Online: 15 January 2021

Priyanka Saha, Rupali Rakshit, and Kalyan Mandal

Journal of Applied Physics ARTICLE scitation.org/journal/jap

Shear response of magnetorheological fluid with $Zn_{0.2}Fe_{2.8}O_4$ sub-micron hollow spheres

Cite as: J. Appl. Phys. **129**, 033901 (2021); doi: 10.1063/5.0031536
Submitted: 1 October 2020 · Accepted: 20 December 2020 ·
Published Online: 15 January 2021

View Online Export Citation CrossMark

Priyanka Saha,[1,a)] Rupali Rakshit,[2] and Kalyan Mandal[1]

AFFILIATIONS

[1]Department of Condensed Matter Physics and Material Science, S. N. Bose National Centre for Basic Sciences, Block JD, Sector III, Salt Lake, Kolkata 700 106, India
[2]Solid State and Structural Chemistry Unit, Indian Institute of Science (IISc), CV Raman Road, Bengaluru, Karnataka 560012, India

[a)]**Author to whom correspondence should be addressed:** priyankasaha@bose.res.in

ABSTRACT

Magnetorheological (MR) fluids with Fe_3O_4 particles are widely studied nowadays due to their soft magnetic nature, controllable morphology, and better chemical stability as compared to their metallic counterpart. However, they can be even more advantageous under Zn doping with elevated magnetization and hollow configuration with low density, making them more active, stable, and dispersible in the carrier fluid. Here, we report the preparation of MR fluids with $Zn_{0.2}Fe_{2.8}O_4$ sub-micrometer hollow spheres and their steady-state MR response under the application of a magnetic field. The MR fluid follows the Bingham plastic nature with a yielding behavior. The variation of yield stress with the applied magnetic field is explained in the context of a newly developed dipolar interaction model.

I. INTRODUCTION

A magnetorheological (MR) fluid consists of a carrier liquid where nano- to micrometer-sized magnetic particles are well dispersed, and the fluid shows a magnetic field responsive reversible change in viscosity from liquid state to solid-like state.[1–3] Until today, MR fluids have received considerable attention in technological applications such as brake, clutch, dampers, seismic vibrations,[4–5] etc. High concentration and large magnetic saturation (M_S) of the suspended magnetic particles in MR fluids improve the magnetorheological response. However, MR response is not always proportional to the particle concentration and rather deteriorates when the particle concentration goes beyond a certain limit.[6] Therefore, to improve MR response, the metallic magnetic particles with high M_S, such as carbonyl iron, are used. However, poor sedimentation stability in suspension due to their high density and poor oxidative stability recommend the use of additives[2,3] and coating.[7–10] Nonetheless, due to additives and coatings, the MR response gets compromised[11] and noneconomic.[12] On the other hand, spinel ferrites with excellent chemical stability and low density are found to be a stable MR material with good magnetorheological response comparable to metallic particles.[13,14] They can be even more advantageous if used in the form of hollow structures that can improve their stability further by reducing the density. MR fluids containing hollow spherical Fe_3O_4 particles were reported earlier.[15,16] Ferrite hollow spheres with good chemical, physical, and sedimentation stability make an excellent MR material both for application purpose and for basic understanding[17] of the MR effect.

In our previous work, we observed Zn doping to improve the magnetization of $Zn_xFe_{3-x}O_4$ hollow spheres up to a certain doping percentage ($x = 0.2$).[18] In this article, $Zn_{0.2}Fe_{2.8}O_4$ (ZFO) hollow spheres with diameter ~700 nm are synthesized via a solvothermal method, and the MR suspension is prepared using them. The steady-state shear response of the MR suspension is studied and explained in detail.

II. EXPERIMENTS AND METHODS

ZFO hollow spheres are prepared following the synthesis procedure as reported earlier.[18] In brief, 1.015 g of $FeCl_3{\cdot}6H_2O$, 0.0315 g of $ZnCl_2$, and 0.46 g of urea are added in 30 ml ethanol and stirred until homogeneous solution is obtained. 25 mg of PVP is added as a surface stabilizer. The properly mixed solution is transferred into a 40 ml Teflon lined stainless steel autoclave and heated at 200 °C for 20 h, followed by natural cooling. The resulting black precipitate is washed with absolute ethanol and dried overnight.

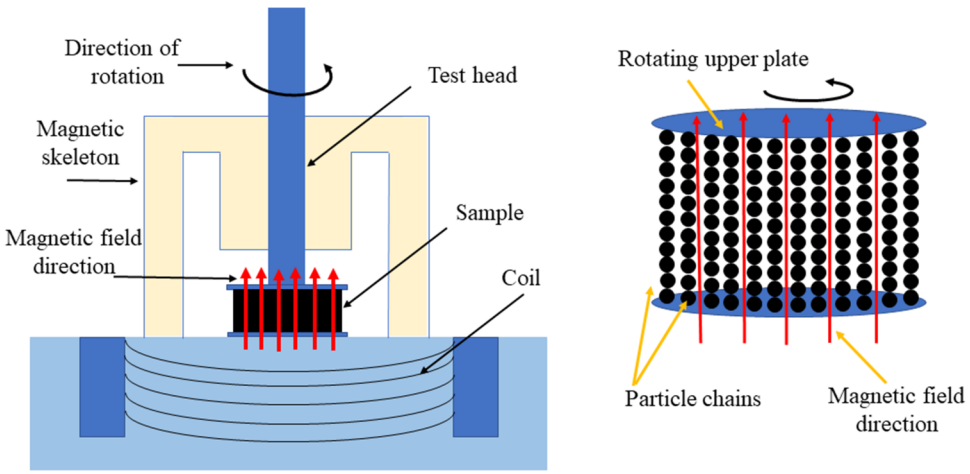

FIG. 1. Left: Schematic diagram of the parallel plate magnetorheometer (MCR 301). Right: Schematic diagram of the particle chain formed in the direction of the magnetic field.

The structure and phase of ZFO hollow spheres are characterized by x-ray diffraction (XRD), while the morphology and elemental analysis are performed by using a scanning electron microscope (SEM) equipped with energy dispersive x-ray spectroscopy (EDX) and a transmission electron microscope (TEM). The magnetic measurements are performed by using a vibrating sample magnetometer at room temperature with a maximum applied field of 10 kOe.

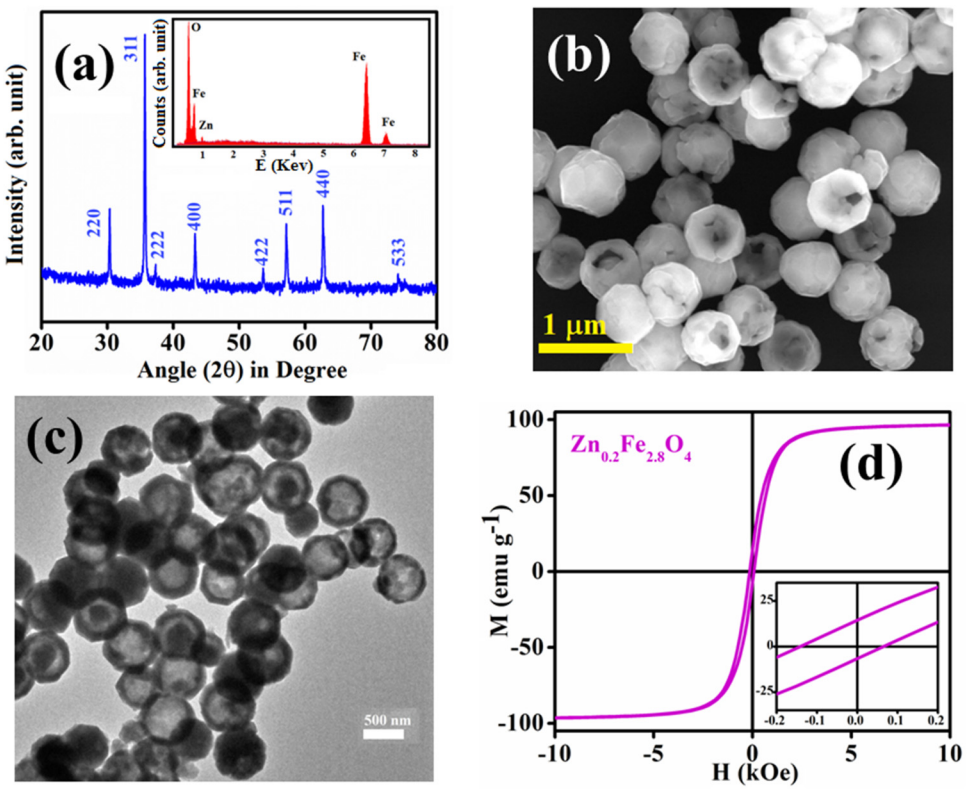

FIG. 2. (a) XRD pattern with EDX spectra (inset), (b) SEM image, (c) TEM image, and (d) room temperature M-H loop of the as-prepared $Zn_{0.2}Fe_{2.8}O_4$ hollow spheres.

The MR fluid with 50 wt. % particle fraction is prepared by adding ZFO hollow spheres in silicone oil (density 0.981 g/cc at room temperature) and henceforth named as ZFO-MR fluid. The mixture is homogenized by mechanical mixing followed by sonication. No additive is present in the prepared MR fluid. The MR measurements are performed in an Anton Parr parallel plate magnetorheometer MCR 301. The gap between two parallel plates is kept at 0.3 mm. A schematic of the magnetorheometer is shown in Fig. 1.

III. RESULTS AND DISCUSSION

The XRD pattern of the as-synthesized sample is shown in Fig. 2(a), which confirms the formation of a single-phase face-centered cubic spinel structure, where the EDX spectra in its inset confirm the element and purity of the as-synthesized material. The SEM image in Fig. 2(b) shows the formation of regular and uniform ZFO spheres of average diameter of 700 nm and rough surface area. Some broken parts of the spheres can also be seen in the SEM image, which confirm the hollow interior of the spheres. The hollow structure of the as-synthesized sample becomes more prominent, from the intensive contrast between the black edge and bright center of the spheres, in the TEM image, as shown in Fig. 2(c), with a shell thickness of 120 nm. Density of the hollow spheres is found to be ~4.9 g/cc, which is much less compared to the density (~5.3 g/cc) of $Zn_{0.2}Fe_{2.8}O_4$ solid spheres. The field-dependent magnetization (M-H) loop in Fig. 2(d) shows soft magnetic nature of ZFO hollow spheres with $M_S = 96$ emu/g, coercivity ~140 Oe, and remanence ~14 emu/g. These magnetic properties suggest that ZFO hollow spheres-based MR fluid will be quick in MR response and re-dispersible due to negligible remanence.

Dispersion stability of the prepared MR fluid is shown in Fig. 3 by plotting the time-dependent sedimentation rate. The MR fluid system is kept steady during the time of stability test. The sedimentation rate is found to be slow as compared to the metallic magnetic particles,[19] which is owed to the low density of ZFO hollow spheres.

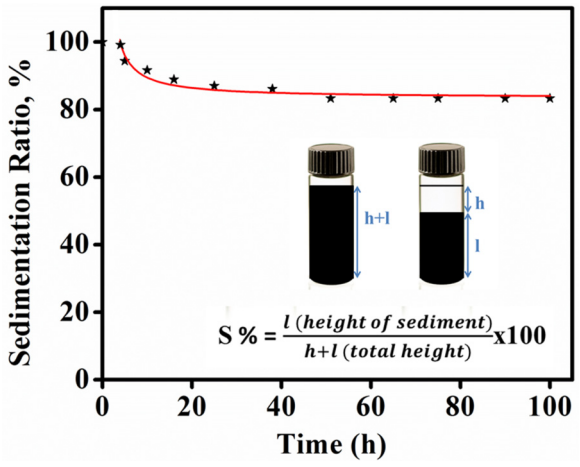

FIG. 3. Sedimentation stability of ZFO-MR fluid with time.

Figure 4(a) exhibits the flow curve of the ZFO-MR fluid and silicon oil only to understand the origin of high shear stress in the MR fluid. The high shear stress of the ZFO-MR fluid even at zero field is due to the rough surface of the hollow spheres which can be observed in the SEM image [Fig. 2(b)]. The shear stress (τ) of the suspension increases in the presence of a magnetic field (H), with the appearance of dynamic yield stress, owing to the formation of magnetic field-induced columnar structures. During the flow test, the measurement is repeated for a particular applied magnetic field, and the flow curve follows the same path each time, proving the negligible effect of remanence magnetization on MR response. The sample represents a shear thinning behavior at a fixed applied magnetic field, as appeared from Fig. 4(b), where with the increase in shear rate ($\dot{\gamma}$), the columnar structures break and initiate flow in the MR fluid. All the curves show non-Newtonian behavior [Fig. 4(a)] and the presence of yield stress under the application of the magnetic field confirms Bingham plastic (BP) nature following

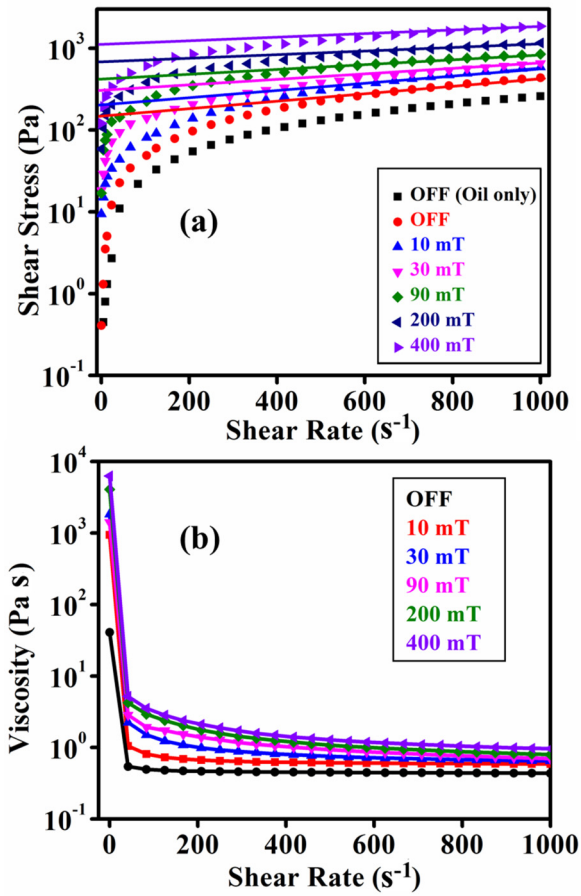

FIG. 4. (a) Steady shear rate flow curve and (b) variation of viscosity with the shear rate of the ZFO-MR fluid.

the BP equation $\tau = \tau_y + \eta\dot{\gamma}$, where τ_y represents the yield stress and η is the plastic viscosity. By extrapolating the shear rate to zero, the yield stress (τ_y) is estimated for different applied magnetic fields. A yield stress (τ_y) of ~1120 Pa is obtained for the maximum applied magnetic field of 400 mT for the ZFO-MR fluid, which is better as compared to the MR fluid with pure Fe_3O_4 hollow spheres.[15] Once the yielding point is reached, the flow curves show gradual increasing nature with the increase in shear rate for all the applied magnetic fields. The slope of this linear region at higher $\dot{\gamma}$ represents the value of plastic viscosity (η), which changes with the applied magnetic field, indicating the dependence of η on the applied field.

To understand the MR mechanism, the nature of variation of the yield stress with the applied magnetic field needs to be studied. In MR fluids, under a weak applied magnetic field, τ_y increases quadratically with increasing magnetic field strength, while at higher values of the applied magnetic field, τ_y is expressed as[20] $\tau_y = \sqrt{6}\phi\mu_0 M_S^{1/2} H^{3/2}$. In the ZFO-MR fluid system, the yielding nature with different magnetic fields does not follow any previously established model as observed from Fig. 5(a). With the externally applied magnetic field, each hollow sphere acts as an individual dipole and forms chain. The nature of variation of τ_y with H is explained by considering frictional force between the hollow spheres and the plates of the magnetorheometer.

Frictional force is proportional to the normal reaction, which is composed of dipolar interaction force between the magnetic particles in the particle chains. Under an applied magnetic field, each sphere acts as a magnetic dipole. The dipolar interaction force between two dipoles can be expressed as

$$F_d = -\frac{3\mu_0 m^2}{2\pi l^4}, \quad (1)$$

where m is the magnetic dipole moment and l is the distance between the particles.

In the MR fluid, the suspended hollow spheres form chain in the direction of the applied magnetic field through dipolar interaction. Considering infinite number of particles in a chain from a lower static plate to an upper rotating plate, as shown in Fig. 5(b), the dipolar interaction force on the hollow sphere in contact with

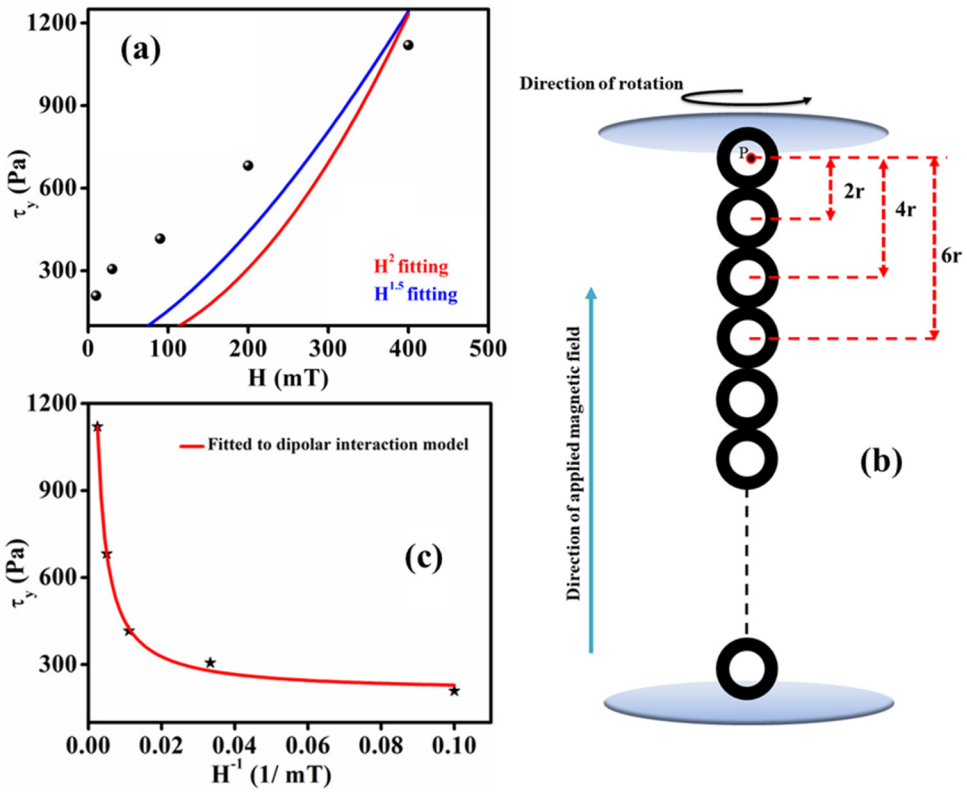

FIG. 5. (a) Variation of yield stress with the applied magnetic field of the ZFO-MR fluid fitted with the previously established standard model. (b) Schematic of infinite particles chain formed due to arising dipole moment under the application of the magnetic field and (c) variation of yield stress with the applied magnetic field of the ZFO-MR fluid fitted with the dipolar interaction model.

the rotating plate can be calculated as

$$F = -\frac{3\mu_0 m^2}{2\pi}\left[\frac{1}{(2r)^4}+\frac{1}{(4r)^4}+\frac{1}{(6r)^4}+\cdots\right], \quad (2)$$

where r is the radius of the ZFO hollow spheres.

By adding the infinite series of Eq. (2), we get

$$F = -\frac{3\mu_0 m^2}{2^5\pi r^4}\frac{\pi^4}{90}. \quad (2a)$$

If we consider a unit volume of length, breadth, and height of unit scale and n number particles per unit length, then there are n^2 number of particles per unit area and n^3 number of particles per unit volume, with n^2 number of particle chains per unit cell. So, the dipolar interaction force per unit area is

$$N = -\frac{3\mu_0 m^2 n^2}{2^5\pi r^4}\frac{\pi^4}{90}. \quad (2b)$$

N is also a normal reaction that is required for calculating the frictional force between the particle chains and the upper plate of the magnetorheometer.

Equation (2b) can be expressed as

$$N = -\frac{3\mu_0 M^2}{2^5\pi r^4 n^4}\frac{\pi^4}{90}, \quad (3)$$

where M is the magnetization of the particles defined as $M = mn^3$.

The normal reaction of Eq. (3) gives rise to frictional force, which in turn develops shear in the ZFO-MR fluid. In the range of the applied magnetic field (400 mT), the ZFO hollow spheres are in the approach to saturation region, where M can be

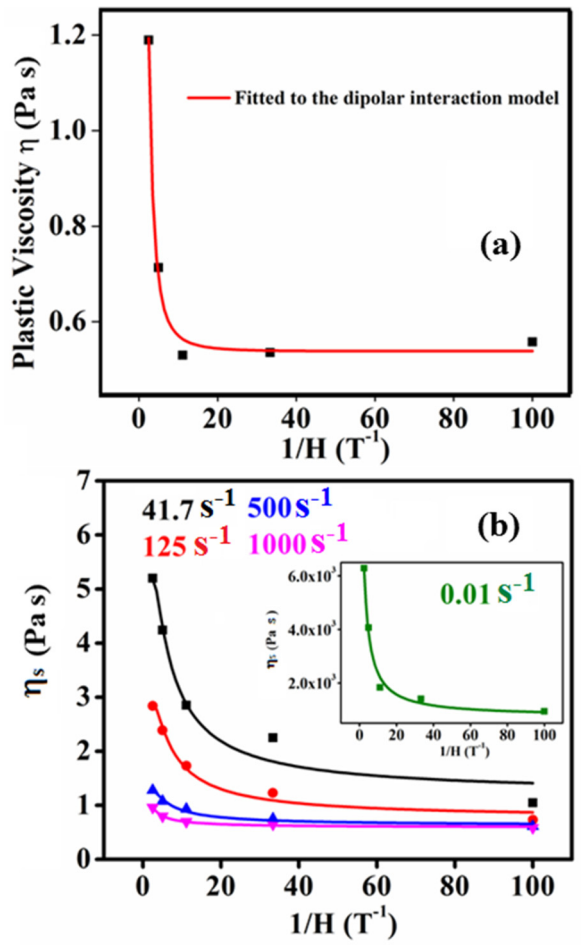

FIG. 6. Nature of variation of (a) plastic viscosity with applied magnetic field intensity and (b) viscosity values at different shear rate η_s with the applied magnetic field at different shear rates of the ZFO-MR fluid; inset figure shows the variation of η_s with 1/H for shear rate 0.01 s^{-1}.

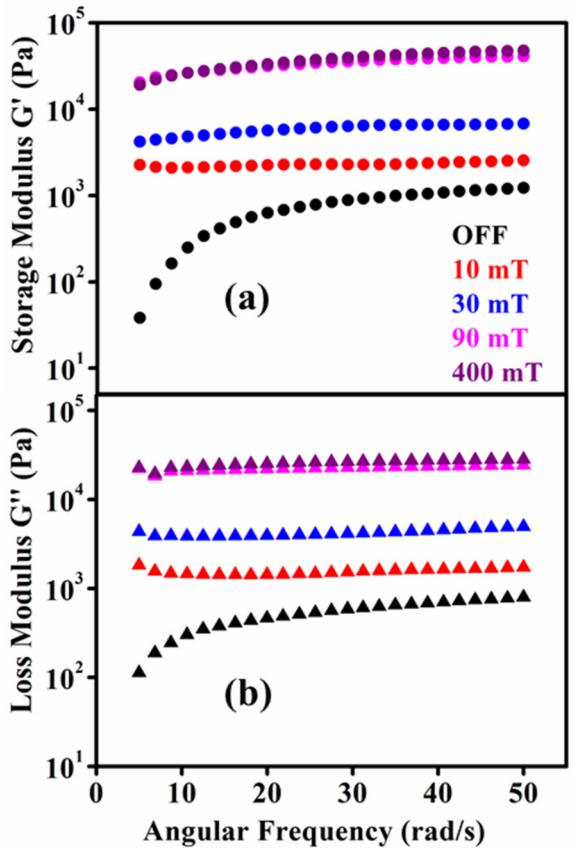

FIG. 7. Variation of (a) storage modulus and (b) loss modulus with angular frequency of the oscillating strain at different applied magnetic fields.

written as[21,22]

$$M = M_S\left(1 - \frac{a}{H} - \frac{b}{H^2} - \cdots\right), \quad (4)$$

where a and b are constants. Combining Eqs. (3) and (4) and neglecting the higher order terms, the field dependence of the normal reaction in the approach to saturation region, N_{AS}, can be expressed as

$$N_{AS}\,\alpha\, M_S^2\left(1 - \frac{2a}{H} + \frac{a^2}{H^2}\right). \quad (5)$$

As the normal reaction is the origin of shear stress, the yield stress τ_y should follow the same H dependency. The variation of τ_y with 1/H is shown in Fig 5(c). Plastic viscosity, η, also varies following the same pattern as τ_y with H, as shown in Fig. 6(a). Viscosity values in our experiment are calculated for different values of shear rate 0.01, 41.7, 125, 500, and 1000 s^{-1} with the applied magnetic field and is denoted as η_s. η_s is found to increase with magnetic field strength due to stronger chain formation in the MR fluid, and their nature of variation with H is shown in Fig. 6(b), fitted with Eq. (5).

Frequency-dependent storage modulus (G′) and loss modulus (G″) at constant shear rate amplitude (0.5%) is shown in Fig. 7. G′ increases with the increase in the magnetic field, suggesting strong solid-like behavior over the liquid-like state, which indicates dominating elastic behavior over viscous nature. G″ also shows improvement under field stimuli. It indicates the enhanced dissipative response in addition to improved elasticity, which is a suitable characteristic for dynamic applications.

IV. CONCLUSION

In conclusion, MR fluid with $Zn_{0.2}Fe_{2.8}O_4$ hollow spheres is prepared and its MR effects and sedimentation behavior are studied in detail. The MR fluid not only shows good dispersion stability but achieves sufficient value of yield stress at a low applied field of 400 mT. Magnetic dipolar interaction is found to govern the MR behavior. This MR fluid with dominating elastic behavior over viscous nature in the presence of an applied magnetic field and excellent MR response is suitable for commercial use such as brake, clutch, and MR damper.

ACKNOWLEDGMENTS

The authors acknowledge S. N. Bose National Centre for Basic Sciences for financial support. P. Saha is grateful to the Department of Science and Technology, Government of India for INSPIRE fellowship.

DATA AVAILABILITY

The data that support the findings of this study are available from the corresponding author upon reasonable request.

REFERENCES

[1]A. Hajalilou, S. Amri Mazlan, H. Lavvafi, and K. Shameli, *Field Responsive Fluids as Smart Materials* (Springer, Singapore, 2016).
[2]B. J. Park, K. H. Song, and H. J. Choi, Mater. Lett. **63**, 1350 (2009).
[3]A. Hajalilou, S. A. Mazlan, and S. T. Shila, Mater. Lett. **181**, 196 (2016).
[4]J. D. Carlson and M. R. Jolly, Mechatronics **10**, 555 (2000).
[5]C. Sarkar and H. Hirani, Def. Sci. J. **63**, 408 (2013).
[6]R. C. Bell, D. T. Zimmerman, and N. M. Wereley, *Magnetorheology* (Royal Society of Chemistry, Cambridge, 2013).
[7]Y. D. Liu and H. J. Choi, J. Appl. Phys. **111**, 07B502 (2012).
[8]S. W. Ko, J. Y. Lim, B. J. Park, M. S. Yang, and H. J. Choi, J. Appl. Phys. **105**, 07E703 (2009).
[9]H. S. Jung and H. J. Choi, J. Appl. Phys. **117**, 17E708 (2015).
[10]A. Hajalilou, A. Kianvash, K. Shameli, and H. Lavvafi, Appl. Phys. Lett. **110**, 261902 (2017).
[11]Y. D. Liu, F. F. Fang, and H. J. Choi, Colloid Polym. Sci. **289**, 1295 (2011).
[12]F. F. Fang and H. J. Choi, J. Appl. Phys. **103**, 07A301 (2008).
[13]A. V. Anupama, V. B. Khopkar, V. Kumaran, and B. Sahoo, Phys. Chem. Chem. Phys. **20**, 20247 (2018).
[14]F. F. Fang, J. H. Kim, and H. J. Choi, Polymer **50**, 2290 (2009).
[15]P. Saha, S. Mukherjee, and K. Mandal, J. Magn. Magn. Mater. **484**, 324 (2019).
[16]S. Xuan, L. Hao, and K. C. F. Leung, New J. Chem. **38**, 6125 (2014).
[17]K. Shahrivar, J. R. Morillas, Y. Luengo, H. Gavilan, P. Morales, C. Bierwisch, and J. de Vicente, J. Rheol. **63**, 547 (2019).
[18]P. Saha, R. Rakshit, M. Alam, and K. Mandal, Phys. Rev. Appl. **11**, 024059 (2019).
[19]Y. Tong, X. Dong, and M. Qi, Smart Mater. Struct. **26**, 025023 (2017).
[20]F. F. Fang, Y. D. Liu, H. J. Choi, and Y. Seo, ACS Appl. Mater. Interfaces **3**, 3487 (2011).
[21]C. W. Chen, *Magnetism and Metallurgy of Soft Magnetic Materials*, 1st ed. (North-Holland Publishing Company, 1997), p. 107.
[22]S. Chikazumi, *Physics of Ferromagnetism*, 2nd ed. (Oxford University Press, 2009), p. 503.